Monolithic Thin Film Red LED Active-Matrix Micro-Display by Flip-Chip Technology

Peian Li, Xu Zhang, *Member, IEEE*, Wing Cheung Chong, and Kei May Lau, *Life Fellow, IEEE*

***Abstract*— A monolithic thin film red light emitting diode (LED) active-matrix (AM) micro-display driven by a complementary metal-oxide semiconductor (CMOS) driver is demonstrated. The resolution of the micro-display is 64 × 36, with a 40 μm × 40 μm pixel pitch. Starting from AlGaInP epi-layers grown on GaAs substrates, the monolithic red LED array was fabricated and then integrated with the AM driver using Au/In flip-chip bonding technology. After removal of the GaAs substrate, a crack-free thin film micro-display was realized with a high pixel yield. The thin film red LED AM micro-display delivers a luminance of 2.35 × 10^4 cd/m^2 at full-load conditions and can render images with 4-bit grayscale. This work not only provides a manufacturing-friendly approach for monolithic thin film red LED micro-displays, but also brings the possibility of hybrid integration with blue/green LEDs to achieve full-color LED micro-displays.**

***Index Terms*— Active-matrix, AlGaInP, light emitting diode, micro-display, flip-chip device, thin film device.**

I. Introduction

VIRTUAL reality (VR) and augmented reality (AR) electronics provide attractive immersion and interactive experiences to users in professional training, surgery, entertainment and other interactive scenarios. Micro-displays are one of the core components in VR/AR devices. Unlike displays for televisions and desktops, micro-displays feature very small dimensions (typically < 1 inch), fine pixel pitch and high brightness to meet the requirements of VR/AR devices [1]. Liquid crystal micro-displays such as liquid crystal on silicon (LCoS), are based on the light modulation properties of liquid crystals. They require a power-hungry backlight unit for the severe light loss and the contrast ratio is limited to a low level [2]. While self-emissive devices such as organic light emitting diode (OLED) micro-displays are a more appealing choice than liquid crystal, OLED technology has challenges in terms of efficiency and reliability, especially for blue OLED materials [3]. Alternatively, self-emissive inorganic light emitting diodes (LEDs) offer higher brightness, a shorter response time and a longer working lifetime, and thus have been considered to be a promising option for micro-displays [4].

Manuscript received March 7, 2021; revised April 19, 2021; accepted April 28, 2021. Date of publication May 7, 2021; date of current version May 17, 2021. This work was supported by the Innovation and Technology Fund of Hong Kong under Grant ITS/382/17FP. *(Corresponding author: Kei May Lau.)*

The authors are with the Department of Electronic and Computer Engineering, The Hong Kong University of Science and Technology, Hong Kong (e-mail: pliar@connect.ust.hk; xzhangbj@connect.ust.hk; eeeddie@connect.ust.hk; eekmlau@ust.hk).

Color versions of one or more figures in this letter are available at https://doi.org/10.1109/LPT.2021.3078198.

Digital Object Identifier 10.1109/LPT.2021.3078198

Inorganic LED micro-displays can be monolithically fabricated on LED epi-wafers grown by metal organic chemical vapor deposition (MOCVD). Because the monolithic approach does not involve any pixel-transfer process, small-size and high-resolution micro-displays can be realized [1], [4], [5] with conventional complementary metal-oxide semiconductor (CMOS) technology, leading to a potentially high pixel yield and lower cost compared with pixel-transfer technology [6]. Research into monolithic LED micro-displays started in 2001 [7], and progressed in the following decades in aspects such as high resolution realization [8], flip-chip integration [9], [10] and active-matrix (AM) driving [11], [12]. Most of these works focused on blue or green InGaN LEDs. Due to the inefficient red emission of InGaN LEDs, red micro-LED displays are fabricated using AlGaInP epi-layers grown on GaAs substrates. However, the GaAs substrates are opaque and electrically conductive, making it impossible to fabricate addressable LED pixel arrays on the original growth substrate. Moreover, the red AlGaInP LED epi-layers are usually thick (8-15 μm), which is also challenging for the fabrication of micro-LEDs. Consequently, a feasible technology to fabricate monolithic red LED micro-displays is yet to be established, limiting the applications of LED micro-displays in full-color VR/AR devices.

Multiple works have attempted to overcome the technical issues of monolithic red LED micro-displays. A straightforward solution is to transfer AlGaInP epi-layers onto transparent and insulating sapphire substrates prior to the fabrication of LEDs [13]. Both passive-matrix (PM) [14] and AM [15] red LED micro-displays have been demonstrated using AlGaInP on sapphire epi-wafers. However, a desirable pixel pitch in VR/AR devices should be less than 50 μm, smaller than what was reported in the past. Furthermore, this transfer technology produces an additional epi-layer transfer cost, while light crosstalk among pixels is induced through the transparent substrate [16]. Instead of using a sapphire substrate, thin film red LED micro-displays have been hybridized with a CMOS driver by eutectic bonding of AlGaInP epi-layers [17]. Although this approach can realize high pixel density with less light crosstalk, it is critical to prevent bonding failure induced by strain and high temperature processes during the complicated fabrication after bonding.

In this work, monolithic red LED micro-displays are firstly fabricated on AlGaInP/GaAs epi-wafers, and then integrated with AM CMOS drivers by flip-chip bonding technology. After bonding, removal process of the GaAs substrate is implemented, preventing any possible pixel damage in the complicated post-bonding processes. The thin film AM micro-displays also exhibit limited light crosstalk and high

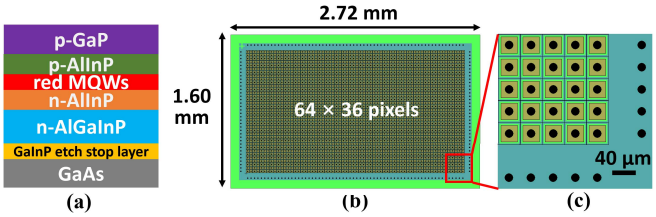

Fig. 1. (a) Structure of the AlGaInP red LED epi-wafers. (b) The layout of the 64 × 36 red LED micro-display and (c) zoomed-in structures of the micro-display, where green, brown, cyan and black represent n-AlGaInP, p-metal on pixels, n-metal and solder bumps, respectively.

luminance. Additionally, this technology is promising for the integration of red AlGaInP LED arrays with blue/green InGaN LED arrays, which is highly challenging for the epi-layer transfer [13]–[15] or epi-layer bonding [17] technologies.

II. Design and Fabrication of Red LED Arrays

Commercially available AlGaInP red LED epi-wafers were grown on 4-inch, 350 μm-thick n-GaAs substrates by MOCVD. Fig. 1 (a) shows the epi-structure composed of a 2 μm p-GaP window layer, 1.2 μm p-AlInP cladding layer, 0.5 μm AlGaInP multiple quantum well (MQW) active layer, 0.7 μm n-AlInP cladding layer, 3.6 μm n-AlGaInP current spreading layer and 0.3 μm GaInP etch stop layer, from the top to the GaAs substrate. The epi-wafer is designed for backside-emitting flip-chip red LEDs. It does not include a distributed Bragg reflector, but has a GaInP layer on the GaAs substrate as an etch stop layer. The etching process stops at the GaAs/GaInP interface when the substrate is removed by wet etching [18], [19].

The layout of the red LED array is illustrated in Fig. 1(b). The size of each chip is 2.72 mm × 1.60 mm, with a resolution of 64 × 36 pixels. The common n-electrode of the pixels is located at the periphery of the display chip. Fig. 1(c) shows the zoomed-in view of the layout. Each pixel has a 40 μm × 40 μm pitch and a 30 μm × 30 μm emitting area. P-electrodes cover the top p-GaP on the pixels, serving as reflectors to improve the backside emission. N-electrodes are on the n-AlGaInP layer, forming a lateral electrode structure. An n-metal grid is deposited in the gaps between pixels to help spread the current via the common n-electrodes, thus maintaining uniform forward voltages across the LED array. Indium solder bumps are formed both on the p-electrodes and n-electrodes for the flip-chip bonding with the AM drivers.

The AlGaInP red LED array was processed using standard microelectronic fabrication technologies. First, 120 nm of Au was deposited as the p-electrode metal on the p-GaP by e-beam evaporation. Next, 1 μm of SiO_2 was deposited by plasma-enhanced chemical vapor deposition (PECVD) on the Au layer as an etching mask. The SiO_2 mask was then selectively patterned in buffered oxide etchant (BOE) to define the emitting area of each pixel. To form the mesa pixel structure shown in Fig. 2 (a), the Au layer under the SiO_2 mask was patterned in diluted KI-I_2 solution. Using the same SiO_2 mask, the AlGaInP red epi-wafer was dry etched in $BCl_3/Cl_2/Ar$ plasma to form 5 μm deep mesas. The Au p-electrodes have high reflectance over the red range (>600 nm) [20], thereby serving as good reflectors in the backside-emitting red LED devices. After removal of the SiO_2

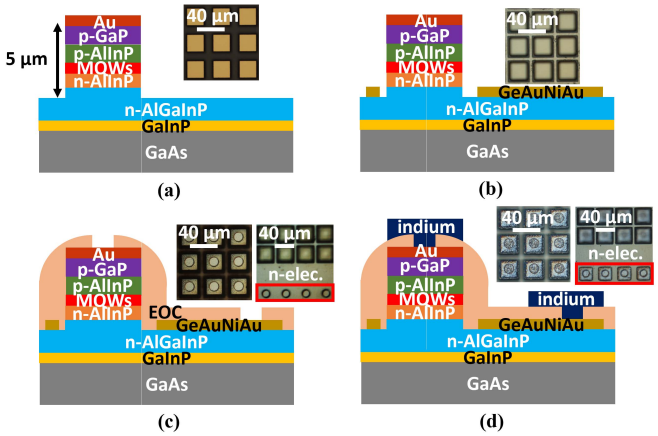

Fig. 2. Cross-sections and photomicrographs of the AlGaInP red LED array illustrating the fabrication process: (a) p-electrode deposition and mesa etching, (b) n-electrode deposition, (c) polymer passivation coating and contact hole opening, and (d) indium pattern deposition.

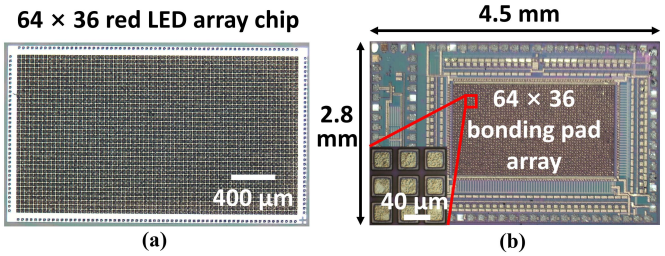

Fig. 3. (a) The entire red LED array after fabrication. (b) The CMOS AM driver with an additional Ti/Au bilayer.

mask, a Ge/Au/Ni/Au (40/40/24/100 nm) metal stack was deposited on the exposed n-AlGaInP as n-electrodes. Both n- and p- electrodes were annealed at 430 °C in nitrogen to form ohmic contact (Fig. 2(b)). EOC, a commercial transparent overcoat photoresist, was coated and patterned as a polymer passivation layer for the LED pixels [21], leaving 15 μm-diameter contact holes on the p- and n-electrodes for the indium solder bumps (Fig. 2(c)). The EOC layer was cured after post-baking at 150 °C for 30 minutes. 2 μm-thick, 30 μm × 30 μm indium patterns were deposited on contact holes as the solder metal for the flip-chip bonding process (Fig. 2(d)).

III. Integration With AM Drivers

A photomicrograph of the red LED array chip after the fabrication process is shown in Fig. 3(a) and it is well in accordance with the layout design (Fig. 1(b, c)). The AM drivers were fabricated using a 0.18 μm bulk CMOS process by a foundry. They were originally designed for InGaN LED micro-displays and can also be used for AlGaInP red LED micro-displays. The details of the working principles and the application are described in our previous publications [10], [22]. The bonding pads on the driver chip fabricated by the CMOS process are Al, which has poor adhesion with indium. Therefore, a Ti/Au bilayer (20/120 nm) was deposited on the bonding pad array (Fig. 3 (b)) by e-beam evaporation. Au/In flip-chip bonding can provide sufficient strength since they form an alloy at a temperature slightly above the melting point of indium. Ti enhances the adhesion between Al and Au, and stops the diffusion of Au at elevated bonding temperatures.

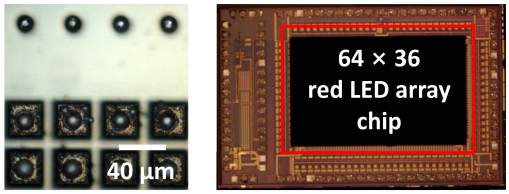

Fig. 4. (a) Indium solder bumps formed by the reflow process. (b) The red LED array integrated with the CMOS AM driver by flip-chip bonding, before removal of the GaAs substrate.

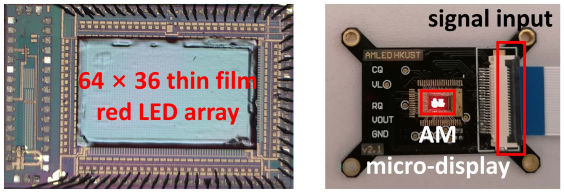

Fig. 5. (a) The monolithic thin film red LED AM micro-display after removal of the GaAs substrate. (b) The driving PCB for the micro-display demo.

Before the flip-chip bonding, a 10-second reflow process was performed for the evaporated indium patterns to form soldering bumps at 180 °C, with the aid of water-soluble soldering flux in a formic acid atmosphere. Because indium does not adhere to the EOC polymer layer, it spontaneously flowed into the contact holes driven by surface tension and was reshaped into indium bumps. The heights of the indium bumps were 8-10 μm, sufficient to offset the 5 μm height difference between the p- and n-electrodes. Thicker bonding pads can be deposited on the n-electrodes of the CMOS driver, thus further offsetting the height difference in the future work. Fig. 4 (a) provides an inspection photomicrograph of uniformly distributed indium solder bumps on the p- and n-electrodes. After the reflow process, the red LED array chip was flip-chip bonded to the AM driver (Fig. 4 (b)) under a bonding force of 10 N at 180 °C for 1 minute in a formic acid atmosphere.

To obtain a thin film LED micro-display, the 350 μm-thick opaque GaAs substrate must be removed after the flip-chip bonding. An ammonia/H_2O_2 mixture is widely used to etch thick GaAs [18], [19]. It is selective to GaInP, so the etching process terminates at the GaAs/GaInP interface. However, this etchant is highly reactive to most metals. To protect the underlying driver and LED pixels, the periphery of the LED chip and the AM driver was covered by photoresist. The photoresist was hard-baked at 120 °C for at least 30 minutes to enhance the adhesion and strength. The integrated micro-display with photoresist protection was etched in the ammonia/H_2O_2 for approximately 1 hour until a smooth, mirror-like GaInP surface was exposed. Fig. 5(a) shows the thin film micro-display after removal of the substrate. The red LED epi-layer is crack-free and firmly adheres to the CMOS driver despite slight deformation at the edge regions, where no bonding bumps exist underneath. Underfill technology can be used in the future work to improve the reliability of solder bumps and minimize the deformation.

Fig. 5(b) illustrates the driving setup for the thin film red LED AM micro-display. The micro-display was fixed on the driving printed circuit board (PCB) with Al wire bonding.

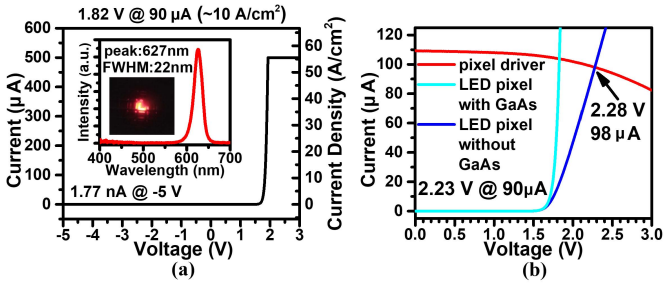

Fig. 6. (a) Typical *I-V* characteristics of red LED pixels (with GaAs substrates) after p- and n-electrode deposition. The inset is the emission photomicrograph of a single pixel and the EL spectrum. (b) The *I-V* characteristics of red LED pixels with/without GaAs substrates and the output characteristics of the pixel driver.

The display controller is an Arduino-based board and all the control signals are sent to the driving PCB via a flexible cable. The monolithic thin film red LED AM micro-display can be demonstrated on this driving platform.

IV. Results and Discussion

Fig. 6(a) plots representative *I-V* characteristics of a single red LED pixel after deposition of the n- and p-electrodes. The forward voltage is 1.82 V at 90 μA (~10 A/cm^2) and 1.92 V at 450 μA (~50 A/cm^2), showing reasonable contact resistances and turn-on performance of the p- and n-electrodes. The reverse leakage current is 1.77 nA at -5 V. The inset shows the electroluminescence (EL) spectrum and the emission image of a red LED pixel. The peak emission is 627 nm with a full width at half maximum (FWHM) of 22 nm.

To estimate the *I-V* characteristics of thin film LED pixels on the CMOS driver, the LED array was flip-chip bonded on a test carrier that had a similar layout to the CMOS driver. The *I-V* characteristics were measured after removal of the GaAs substrate. Fig. 6(b) plots the *I-V* characteristics of the LED pixels with and without the GaAs substrate. After removal of the GaAs substrate, the forward voltage of the thin film LED pixels is 2.23 V at 90 μA (~10 A/cm^2), which represents an increase of 0.41 V. The curve becomes more linear rather than exponential, implying that the series resistance of the LEDs increases somewhat. This indicates that the driving current of the original LED pixels mainly passes through the thick, highly conductive n-GaAs substrate. In the thin film LEDs without GaAs, the driving current must move laterally through the 3 μm-thick n-AlGaInP layer, leading to a higher series resistance. Despite this, the operating voltage of the LED pixels still lies within an acceptable range.

The output current of the AM pixel driver when driving the thin film red LED pixels was estimated. The schematic design of the AM pixel driver is illustrated in our previous publication [22]. The supply voltage of the AM pixel driver was measured to be 3.32 V. The pixel driver and the LED pixels are serially connected, and thus the increase in the operating voltage of the LED leads to a decrease in the driving current, as shown in the output characteristics of the pixel driver plotted in Fig. 6(b). The operation point of the thin film LED pixels is around 2.28 V and 98 μA (~11 A/cm^2). The total power consumption of the thin film red LED array is 0.5 W under full-load conditions, and the luminance is about 2.35 × 10^4 cd/m^2. The micro-display has the potential

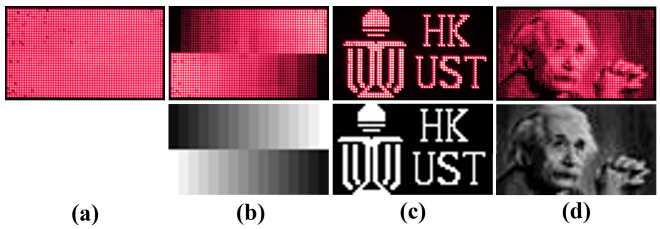

Fig. 7. The images (the upper half) displayed on the monolithic thin film red LED AM micro-display and the original image sources (the bottom half): (a) all lit-up, (b) stripes with 4-bit grayscale, (c) simple patterns/texts and (d) the portrait image.

to achieve a luminance of over 10^5 cd/m^2 at higher driving current density.

Images rendered by the monolithic thin film red LED AM micro-display are demonstrated in Fig. 7. All pixels were connected to the driver and powered up. The all-lit-up image (Fig. 7 (a)) indicates a uniform emission over the whole display area. Some pixels, especially those at the edge region, are darker than the others due to poor contact of solder bumps. It will be improved by applying a more uniform bonding force when performing flip-chip bonding. The stripe patterns (Fig. 7 (b)) clearly show the capability of 4-bit grayscale control. The patterns/texts on a black background (Fig. 7 (c)) demonstrate that there is no significant light crosstalk problem compared with flip-chip LED micro-displays with sapphire substrates [10]. The portrait image (Fig. 7 (d)) proves that the micro-display can provide good visual effects and present sufficient details.

V. Conclusion

A monolithic thin film red LED AM micro-display is demonstrated in this work. The resolution of the micro-display is 64 $\times$ 36 pixels with a 40 μm pixel pitch. The red LED array was monolithically fabricated starting from commercial AlGaInP epi-layers grown on GaAs substrates. The red LEDs have a lateral electrode structure, and they were integrated with an AM micro-display driver by Au/In flip-chip bonding. The opaque GaAs substrate was removed by a wet etching process, leaving the backside-emitting thin film red LED pixels on the driver. The thin film red LEDs are crack-free and the bonding yield is high. The display performance of the micro-display was evaluated on our driving platform. It presents a luminance of 2.35 $\times$ 10^4 cd/m^2 under full-load conditions, with a 0.5 W power consumption of the LED array. Images shown with 4-bit grayscale prove the display capability of this red LED micro-display and the feasibility of practical applications. This work provides a simple, cost-effective approach for monolithic thin film red LED micro-displays, suggesting tremendous potential for integrating red AlGaInP LEDs with blue/green InGaN LEDs to realize full-color micro-displays.

References

[1] T. Jung, J. H. Choi, S. H. Jang, and S. J. Han, "32-1: Invited paper: Review of micro-light-emitting-diode technology for micro-display applications," in *SID Dig. Tech. Pap.*, Jun. 2019, vol. 50, no. 1, pp. 442–446, doi: 10.1002/sdtp.12951.

[2] Y. Huang, E. Liao, R. Chen, and S.-T. Wu, "Liquid-crystal-on-silicon for augmented reality displays," *Appl. Sci.*, vol. 8, no. 12, p. 2366, Nov. 2018, doi: 10.3390/app8122366.

[3] J.-H. Lee *et al.*, "Blue organic light-emitting diodes: Current status, challenges, and future outlook," *J. Mater. Chem. C*, vol. 7, no. 20, pp. 5874–5888, May 2019, doi: 10.1039/c9tc00204a.

[4] T. Wu *et al.*, "Mini-LED and micro-LED: Promising candidates for the next generation display technology," *Appl. Sci.*, vol. 8, no. 9, p. 1557, Sep. 2018, doi: 10.3390/app8091557.

[5] X. Zhou *et al.*, "Growth, transfer printing and colour conversion techniques towards full-colour micro-LED display," *Prog. Quantum Electron.*, vol. 71, May 2020, Art. no. 100263, doi: 10.1016/j.pquantelec.2020.100263.

[6] J. Li, B. Luo, and Z. Liu, "Micro-LED mass transfer technologies," in *Proc. 21st Int. Conf. Electron. Packag. Technol. (ICEPT)*, Aug. 2020, pp. 1–3, doi: 10.1109/ICEPT50128.2020.9201923.

[7] H. X. Jiang, S. X. Jin, J. Li, J. Shakya, and J. Y. Lin, "III-nitride blue microdisplays," *Appl. Phys. Lett.*, vol. 78, no. 9, pp. 1303–1305, Feb. 2001, doi: 10.1063/1.1351521.

[8] W. C. Chong, W. K. Cho, Z. J. Liu, C. H. Wang, and K. M. Lau, "1700 pixels per inch (PPI) passive-matrix micro-LED display powered by ASIC," in *Proc. IEEE Compound Semiconductor Integr. Circuit Symp. (CSICS)*, Oct. 2014, pp. 1–4, doi: 10.1109/CSICS.2014.6978524.

[9] Z. J. Liu, W. C. Chong, K. M. Wong, and K. M. Lau, "360 PPI flip-chip mounted active matrix addressable light emitting diode on silicon (LEDoS) micro-displays," *J. Display Technol.*, vol. 9, no. 8, pp. 678–682, Aug. 2013, doi: 10.1109/jdt.2013.2256107.

[10] X. Zhang *et al.*, "Active matrix monolithic LED micro-display using GaN-on-Si epilayers," *IEEE Photon. Technol. Lett.*, vol. 31, no. 11, pp. 865–868, Jun. 1, 2019, doi: 10.1109/lpt.2019.2910729.

[11] X. Li *et al.*, "Design and characterization of active matrix LED microdisplays with embedded visible light communication transmitter," *J. Lightw. Technol.*, vol. 34, no. 14, pp. 3449–3457, Jul. 15, 2016, doi: 10.1109/jlt.2016.2562667.

[12] C. J. Chen, H. C. Chen, J. H. Liao, C. J. Yu, and M. C. Wu, "Fabrication and characterization of active-matrix 960 $\times$ 540 blue GaN-based micro-LED display," *IEEE J. Quantum Elect.*, vol. 55, no. 2, Apr. 2019, Art. no. 3300106, doi: 10.1109/JQE.2019.2900540.

[13] R.-H. Horng, H.-Y. Chien, K.-Y. Chen, W.-Y. Tseng, Y.-T. Tsai, and F.-G. Tarntair, "Development and fabrication of AlGaInP-based flip-chip micro-LEDs," *IEEE J. Electron Devices Soc.*, vol. 6, pp. 475–479, 2018, doi: 10.1109/jeds.2018.2823981.

[14] R.-H. Horng, H.-Y. Chien, F.-G. Tarntair, and D.-S. Wuu, "Fabrication and study on red light micro-LED displays," *IEEE J. Electron Devices Soc.*, vol. 6, pp. 1064–1069, 2018, doi: 10.1109/jeds.2018.2864543.

[15] Z. J. Liu, W. C. Chong, K. M. Wong, K. H. Tam, and K. M. Lau, "A novel BLU-free full-color LED projector using LED on silicon micro-displays," *IEEE Photon. Technol. Lett.*, vol. 25, no. 23, pp. 2267–2270, Dec. 1, 2013, doi: 10.1109/lpt.2013.2285229.

[16] K. H. Li, Y. F. Cheung, C. W. Tang, C. Zhao, K. M. Lau, and H. W. Choi, "Optical crosstalk analysis of micro-pixelated GaN-based light-emitting diodes on sapphire and Si substrates," *Phys. Status Solidi A*, vol. 213, no. 5, pp. 1193–1198, May 2016, doi: 10.1002/pssa.201532789.

[17] L. Zhang, F. Ou, W. C. Chong, Y. Chen, and Q. Li, "Wafer-scale monolithic hybrid integration of Si-based IC and III-V epi-layers—A mass manufacturable approach for active matrix micro-LED micro-displays: Active matrix micro-LED micro displays made with monolithic hybrid integration," *J. Soc. Inf. Display*, vol. 26, no. 3, pp. 137–145, Mar. 2018, doi: 10.1002/jsid.649.

[18] W. C. Peng and Y. S. Wu, "High-power AlGaInP light-emitting diodes with metal substrates fabricated by wafer bonding," *Appl. Phys. Lett.*, vol. 84, no. 11, pp. 1841–1843, Mar. 2004, doi: 10.1063/1.1682696.

[19] R. H. Horng, S. Sinha, C. P. Lee, H. A. Feng, C. Y. Chung, and C. W. Tu, "Composite metal substrate for thin film AlGaInP LED applications," *Opt. Exp.*, vol. 27, no. 8, pp. A397–A403, Apr. 2019, doi: 10.1364/oe.27.00a397.

[20] R. H. Horng *et al.*, "AlGaInP light-emitting diodes with mirror substrates fabricated by wafer bonding," *Appl. Phys. Lett.*, vol. 75, no. 20, pp. 3054–3056, Nov. 1999, doi: 10.1063/1.125228.

[21] X. Zou, Y. Cai, W. C. Chong, and K. M. Lau, "Fabrication and characterization of high-voltage LEDs using photoresist-filled-trench technique," *J. Display Technol.*, vol. 12, no. 4, pp. 397–401, Apr. 2016, doi: 10.1109/JDT.2015.2493368.

[22] J. Jiang *et al.*, "Fully-integrated AMLED micro display system with a hybrid voltage regulator," in *Proc. IEEE Asian Solid-State Circuits Conf. (A-SSCC)*, Nov. 2017, pp. 277–280, doi: 10.1109/ASSCC.2017.8240270.